

# Calculations of binding affinity between C8-substituted GTP analogs and the bacterial cell-division protein FtsZ

Jozef Hritz · Tilman Läppchen · Chris Oostenbrink

Received: 1 April 2010 / Revised: 21 May 2010 / Accepted: 26 May 2010 / Published online: 18 June 2010  
© The Author(s) 2010. This article is published with open access at Springerlink.com

**Abstract** The FtsZ protein is a self-polymerizing GTPase that plays a central role in bacterial cell division. Several C8-substituted GTP analogs are known to inhibit the polymerization of FtsZ by competing for the same binding site as its endogenous activating ligand GTP. Free energy calculations of the relative binding affinities to FtsZ for a set of five C8-substituted GTP analogs were performed. The calculated values agree well with the available experimental data, and the main contribution to the free energy differences is determined to be the conformational restriction of the ligands. The dihedral angle distributions around the glycosidic bond of these compounds in water are known to vary considerably depending on the physicochemical properties of the substituent at C8. However, within the FtsZ protein, this substitution has a negligible influence on the dihedral angle distributions, which fall within the narrow range of  $-140^\circ$  to  $-90^\circ$  for all investigated compounds. The

corresponding ensemble average of the coupling constants  $^3J(C4,H1')$  is calculated to be  $2.95 \pm 0.1$  Hz. The contribution of the conformational selection of the GTP analogs upon binding was quantified from the corresponding populations. The obtained restraining free energy values follow the same trend as the relative binding affinities to FtsZ, indicating their dominant contribution.

**Keywords** GTP analogs · FtsZ · One-step free energy perturbation · Conformational selection · Restraining free energy · Ensemble average · Heteronuclear coupling constant

## Introduction

The cell division protein FtsZ is considered a promising antibacterial target (Vollmer 2006; Huang et al. 2007; Paradis-Bleau et al. 2007; Lock and Harry 2008; Kapoor and Panda 2009), and the recent discovery of a small synthetic FtsZ inhibitor with potent in vitro and in vivo bactericidal activity against multidrug-resistant *Staphylococcus aureus* suggests that these high expectations are justified (Haydon et al. 2008; Czaplewski et al. 2009).

In the presence of guanosine 5'-triphosphate (GTP), FtsZ assembles into a variety of polymeric structures, the nature of which is very much dependent on the exact experimental conditions employed (reviewed by Adams and Errington 2009). Linear protofilaments and protofilament bundles arising from lateral association are among the more frequently studied polymeric species of FtsZ. Polymerization of FtsZ activates its GTPase activity by insertion of acidic residues from the synergy loop into the nucleotide binding pocket of the preceding monomer in the protofilament (Oliva et al. 2004). Despite considerable

J. Hritz · C. Oostenbrink (✉)  
Leiden-Amsterdam Center for Drug Research,  
Section of Molecular Toxicology,  
Department of Chemistry and Pharmacology,  
Vrije Universiteit, De Boelelaan 1083,  
1081 HV Amsterdam, The Netherlands  
e-mail: c.oostenbrink@few.vu.nl

J. Hritz  
e-mail: jozef.hritz@gmail.com

T. Läppchen  
Department of Biomolecular Engineering,  
Philips Research, High Tech Campus 11,  
M/S WBC02 P263, 5656 AE Eindhoven, The Netherlands  
e-mail: tilman.lappchen@philips.com

C. Oostenbrink  
Institute of Molecular Modeling and Simulation,  
University of Natural Resources and Applied Life Sciences,  
Muthgasse 18, 1190 Vienna, Austria

efforts, FtsZ polymer dynamics, the associated GTPase reaction kinetics, and the modulation of both by pH, nature and concentration of cations, GTP, guanosine 5'-diphosphate (GDP), FtsZ, and certainly regulation by accessory proteins is still not fully understood at a molecular level (Löwe and Amos 1998; Michie and Lowe 2006; Mendieta et al. 2009). In particular, the relationship between GTP hydrolysis and FtsZ polymer dynamics remains controversial. While earlier studies suggested direct exchange of nucleotide in protofilaments (Romberg and Mitchison 2004; Tadros et al. 2006), recent data show that terminal FtsZ subunit exchange is independent of nucleotide state and faster than GTP hydrolysis, supporting the hypothesis that nucleotide exchange occurs only on recycling terminal subunits (Chen and Erickson 2009). In addition, the previously accepted view that the GTP-bound form of the FtsZ protofilament is intrinsically straight while the GDP-bound form is curved has recently been challenged by the finding that FtsZ structures in various crystal forms and nucleotide states did not show evidence of a conformational switch in the FtsZ monomer involving domain movement (Oliva et al. 2007), although it should be taken into account that the crystal structures might not be representative for the GTP- or GDP-bound state but in fact could correspond to a transition state. Strikingly, even 8-morpholino-GTP, one of a series of C8-substituted GTP analogs acting as competitive inhibitors of GTP-driven FtsZ polymerization and GTP hydrolysis, was found to bind to *Aquifex aeolicus* FtsZ in essentially the same way as GDP without inducing any significant conformational changes in the protein (Läppchen et al. 2008). Until now, the molecular basis of the observed inhibitory action of the investigated C8-substituted GTP derivatives has not been completely resolved. Although the C8-morpholino substituent protrudes from the surface of the monomer, the currently available FtsZ protofilament structures (Oliva et al. 2004, 2007) suggest that the inhibitory action cannot be simply attributed to direct steric clashes between the C8 substituent and the next FtsZ monomer in a growing protofilament. It is important to note, however, that stabilization of intersubunit contacts and the rate of GTPase activity are also dependent on the presence of divalent and monovalent cations and pH (Mendieta et al. 2009), suggesting that the C8-substituted GTP derivatives might act by interfering with vital hydrogen-bonding interactions via rearrangement of water molecules and cations in the active site.

In a series of C8-substituted GTP analogs, inhibitory potencies were found to correlate with the corresponding binding affinities to the FtsZ monomer and with the Sterimol parameters of their C8 substituents (Läppchen et al. 2008). Intrigued by this observation, we set out to rationalize these results in terms of binding free energies. C8-substituted GTP analogs with two stable conformations

(*anti*, *syn*) separated by high energy barriers belong to a challenging class of compounds for binding affinity calculations (Hritz and Oostenbrink 2007, 2008). Recently we have developed the enhanced sampling one-step free energy perturbation method (ES-OS) that allows for efficient free energy calculations for GTP analogs in explicit solvent based on sufficient sampling of both relevant conformations (Hritz and Oostenbrink 2009).

This paper presents calculations of relative free energies of binding to the FtsZ protein for a set of five C8-substituted GTP analogs in which H8 is replaced by halogen atoms or a methyl group (Fig. 1). Molecular docking simulations of the C8-substituted GTP analogs well reproduced the phosphate and ribose groups of the molecules, while the base was found to be in both the *syn* and the *anti* conformation (Läppchen 2007). The recent high-resolution crystal structure of the *Aquifex aeolicus* FtsZ protein, co-crystallized with 8-morpholino-GTP, shows that also compounds with a bulky substituent at the C8 position bind to the protein in the *anti* conformation (Läppchen et al. 2008), even though in solution the *syn* conformation is expected to be dominant (Davies 1978; Stolarski et al. 1984; Cho and Evans 1991). This observation significantly simplifies the free energy calculations of the compounds in the binding site of the FtsZ protein, because the simulation can be restricted to a single ligand conformation and no high energy barriers need to be crossed. For this reason we calculate the free energy difference between the various compounds bound to the FtsZ protein using the one-step (OS) perturbation method (Liu et al. 1996; Oostenbrink and van Gunsteren 2005). The corresponding values in solution (where both *anti* and *syn* conformations contribute) were calculated earlier using enhanced sampling OS (ES-OS) (Hritz and Oostenbrink 2009).

The computationally predicted values are compared with the available experimental binding affinities to nucleotide-free *Methanococcus jannaschii* FtsZ protein (Läppchen et al. 2008). The main contributions to the

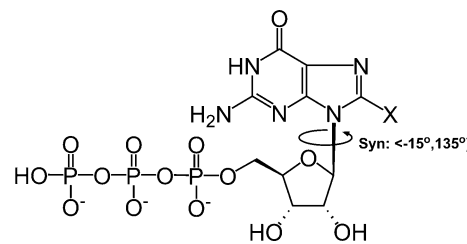


**Fig. 1** Structure of C8-substituted analogs of GTP in *syn* conformation, where  $X = H, F, Cl, Br, CH_3$ . Conformational transitions between the *syn* and *anti* conformations occur by rotation around the glycosidic bond indicated by the arrow. The glycosidic dihedral angle ( $\gamma$ ) is defined over atoms: C4-N9-C1'-O4'

relative binding free energies are analyzed and provide an explanation for the empirically observed correlation between Sterimol parameters of C8 substituents and binding affinities (Läppchen et al. 2008).

## Materials and methods

### One-step free energy perturbation (OS) (Liu et al. 1996)

The aim of OS is to efficiently determine the free energy differences between chemically similar compounds from a single molecular dynamics (MD) simulation of a designed reference compound,  $S$ . The free energy between the reference compound ( $S$ ) and the real compounds ( $R$ ), can be calculated from a simulation using the reference Hamiltonian and applying Zwanzig's perturbation formula (Zwanzig 1954):

$$\Delta G_{SR} = G_R - G_S = -k_B T \ln \left\langle e^{\frac{-(H_R(\mathbf{q}, \mathbf{p}) - H_S(\mathbf{q}, \mathbf{p}))}{k_B T}} \right\rangle_S \quad (1)$$

where  $k_B$  is the Boltzmann constant,  $T$  is absolute temperature, and  $H_S$  and  $H_R$  are the Hamiltonians for the (soft) reference compound and one of the real compounds, respectively. The angular brackets indicate an ensemble average over the positions,  $\mathbf{q}$ , and momenta,  $\mathbf{p}$ , obtained from a simulation of the reference state.

The ensemble average  $\langle A \rangle^R$  of a property  $A$  for the real compound ( $R$ ) can be estimated by reweighting the individual values corresponding to the particular configuration  $(\mathbf{q}_i, \mathbf{p}_i)$  for the reference compound,  $A_i^S$  by a Boltzmann factor  $p_i^{SR}$ :

$$\langle A \rangle^R = \sum_i p_i^{SR} A_i^S; \text{ with } p_i^{SR} = \frac{e^{\frac{-(H_R(\mathbf{q}_i, \mathbf{p}_i) - H_S(\mathbf{q}_i, \mathbf{p}_i))}{k_B T}}}{\sum_i e^{\frac{-(H_R(\mathbf{q}_i, \mathbf{p}_i) - H_S(\mathbf{q}_i, \mathbf{p}_i))}{k_B T}}}. \quad (2)$$

### Simulation setup

The crystal structure of *Aquifex aeolicus* FtsZ complexed with 8-morpholino-GTP (Läppchen et al. 2008) was downloaded from the protein databank (Berman et al. 2003) ([www.pdb.org](http://www.pdb.org); PDB ID: 2R75, chain B). The morpholino substituent was replaced by a single bromine (Br) atom. Molecular dynamics (MD) simulations of the FtsZ protein in complex with 8-Br-GTP were performed using the GROMOS05 simulation package (Christen et al. 2005) in combination with the GROMOS 53A6 force field (Oostenbrink et al. 2004). Force field parameters for five C8-substituted GTP analogs are available in the supplementary material of (Hritz and Oostenbrink 2009). The magnesium cation and all 283 crystallographic water

oxygens were kept and position restrained during initial equilibration steps.

Rectangular periodic boundary conditions were used with an additional 24,544 water molecules; 13 of them were replaced by 13 sodium cations in order to electro-neutralize the whole system (note: crystallographic waters were not considered for replacement by sodium cations). The system finally contained 24,814 explicit simple point charge (SPC) water molecules (Berendsen et al. 1981). All bonds were constrained, using the SHAKE algorithm (Ryckaert et al. 1977), with relative geometric accuracy of  $10^{-4}$ , allowing for a time step of 2 fs in the leapfrog integration scheme (Hockney 1970). After a steepest-descent minimization to remove bad contacts between molecules, initial velocities were randomly assigned from a Maxwell–Boltzmann distribution at 298 K, according to the atomic masses. The temperature was kept constant using weak coupling (Berendsen et al. 1984) to a bath of 298 K with a relaxation time of 0.1 ps. The solute molecule and solvent were independently coupled to the heat bath. The pressure was controlled using isotropic weak coupling to atmospheric pressure (Berendsen et al. 1984) with a relaxation time of 0.5 ps. van der Waals and electrostatic interactions were calculated using a triple range cutoff scheme. Interactions within a short-range cutoff of 0.8 nm were calculated every time step from a pair list that was generated every five steps. At these time points, interactions between 0.8 and 1.4 nm were also calculated and kept constant between updates. A reaction-field contribution was added to the electrostatic interactions and forces to account for a homogeneous medium outside the long-range cutoff, using the relative permittivity (61) of SPC water (Tironi et al. 1995). Selected interactions were calculated using a soft-core van der Waals and electrostatic interaction between atoms  $i$  and  $j$  (Beutler et al. 1994):

$$E_{ij}^{\text{vdw}}(r_{ij}, \lambda_{\text{vdw}}) = \left( \frac{C12_{ij}}{A_{ij}(\lambda_{\text{vdw}}) + r_{ij}^6} - C6_{ij} \right) \frac{1}{A_{ij}(\lambda_{\text{vdw}}) + r_{ij}^6}, \quad (3)$$

$$E_{ij}^{\text{el}}(r_{ij}, \lambda_{\text{el}}) = \frac{q_i q_j}{4\pi\epsilon} \frac{1}{\sqrt{B_{ij}(\lambda_{\text{el}}) + r_{ij}^2}}, \quad (4)$$

with  $r_{ij}$  being the interatomic distance;  $A_{ij}(\lambda_{\text{vdw}}) = \alpha_{\text{vdw}} \frac{C12_{ij}}{C6_{ij}} \lambda_{\text{vdw}}^2$  and  $B_{ij}(\lambda_{\text{el}}) = \alpha_{\text{el}} \lambda_{\text{el}}^2$ .  $C12_{ij}$  and  $C6_{ij}$  are the Lennard–Jones parameters for atom pair  $i$  and  $j$ ,  $q_i$  and  $q_j$  are the partial charges of particles  $i$  and  $j$ , and  $\alpha_{\text{vdw}}$  and  $\alpha_{\text{el}}$  are the softness constants. In the current study we used in all simulations  $\alpha_{\text{vdw}} \lambda_{\text{vdw}}^2 = \alpha_{\text{el}} \lambda_{\text{el}}^2 = 0.3775$ , the value empirically known to work well in standard OS (Schäfer et al. 1999; Oostenbrink and van Gunsteren 2004). It can be seen that at longer distances [ $r_{ij} \gg A(\lambda_{\text{vdw}})$  and  $r_{ij} \gg B(\lambda_{\text{el}})$ ] the soft-core interaction approximates the

interaction for normal atoms and that they differ mostly at short distances between the atoms [ $r_{ij} \leq A(\lambda_{\text{vdw}})$  or  $r_{ij} \leq B(\lambda_{\text{cl}})$ ]. The conformational space of the C8-substituted GTP analogs was adequately represented within the FtsZ protein by the reference state 8-soft\_Br-GTP. Here, a bromine substituent was placed at position 8, for which all nonbonded interactions with the rest of the system (including protein and solvent) were evaluated as soft-core interactions (Eq. 3, 4). A single MD simulation of the reference state FtsZ:8-soft\_Br-GTP was performed for 2 ns, and system coordinates were saved every 0.2 ps.

## Results

Figure 2 presents the normalized dihedral angle ( $\chi$ ) distributions for the five C8-substituted analogs of GTP in complex with the FtsZ protein as calculated by reweighting the probabilities of individual configurations of the MD trajectory of the reference state (8-soft\_Br-GTP) using Eq. (2). The distributions indicate that all five studied GTP analogs occupy a very similar conformational range,  $\chi \in [-140^\circ, -90^\circ]$ , when bound to FtsZ. This range is only about half of the *anti* conformational range observed for these compounds free in solution. The rest of the *anti* range is strongly prohibited by steric repulsion of Phe175 and hydrogen bonding with Asp179 in the FtsZ active site. The different glycosidic dihedral angle distributions in the bound and free state have a direct influence on the  ${}^3J$  coupling constant values, calculated as ensemble averages  $\langle {}^3J(\text{C4}, \text{H1}') \rangle^R$  using Eq. 2.  ${}^3J(\text{C4}, \text{H1}')_i^S$  values for the

individual configurations of the reference compound ( $S$ ) were calculated using the Karplus equation (Karplus 1959):

$${}^3J(\text{C4}, \text{H1}')_i^S = A \cos^2(\chi_i + 120^\circ) + B \cos(\chi_i + 120^\circ) + C \quad (5)$$

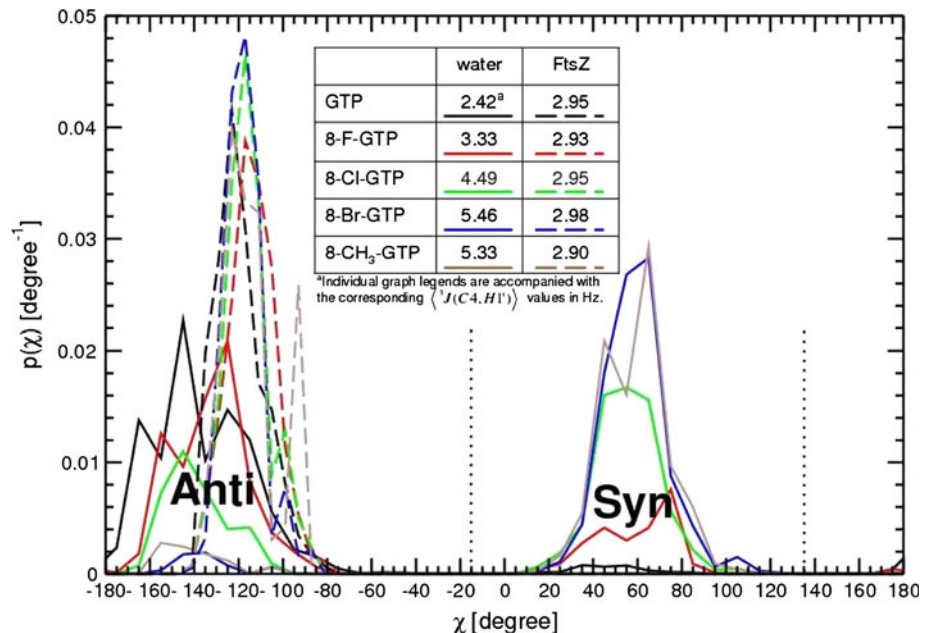
with the Karplus coefficients,  $A = 4.4$  Hz,  $B = -1.4$  Hz, and  $C = 0.1$  Hz (Trantirek et al. 2002). The  ${}^3J$  values for both states are listed in the caption of Fig. 2. While there is a large difference between the calculated  $\langle {}^3J(\text{C4}, \text{H1}') \rangle^R$  values of individual compounds in water, the values are almost identical when bound to the FtsZ protein and fall in the very narrow range of  $2.95 \pm 0.1$  Hz. A separate simulation of real 8-Br-GTP bound to the protein yielded an average  ${}^3J$ -value of 3.01 Hz.

Free energy differences of the five compounds relative to the reference 8-soft\_Br-GTP bound to FtsZ as calculated by OS are listed on the left side of the thermodynamic cycle presented in Fig. 3. The free energies relative to GTP ( $\Delta G_{\text{GTP,R}}^{\text{OS}}(\text{FtsZ})$ ) obtained by cycle closure (right side) are listed in the second column of Table 1. Relative differences in binding affinities,  $\Delta \Delta G_{\text{GTP,R}}^{\text{calc}}(\text{bind})$ , are calculated using Eq. 6.

$$\Delta \Delta G_{\text{GTP,R}}^{\text{calc}}(\text{bind}) = \Delta G_{\text{GTP,R}}^{\text{OS}}(\text{FtsZ}) - \Delta G_{\text{GTP,R}}^{\text{ES-OS}}(\text{aq}), \quad (6)$$

where  $\Delta G_{\text{GTP,R}}^{\text{ES-OS}}(\text{aq})$  are the free energy values relative to GTP in a water environment as calculated by the ES-OS method in our previous study (Hritz and Oostenbrink 2009). It is important to note that, despite the different soft reference states used in water and for the FtsZ bound state, the relative free energy differences between real compounds remain valid for the calculation of relative binding

**Fig. 2** Normalized dihedral angle ( $\chi$ ) distributions for C8-substituted analogs of GTP as calculated by ES-OS in water environment [solid lines (Hritz and Oostenbrink 2009)] and by OS in bound state to FtsZ protein (dashed lines). Ensemble averages of  $\langle {}^3J(\text{C4}, \text{H1}') \rangle$  values in Hz are listed in the legend above individual line symbols. *Anti* and *syn* conformational ranges are indicated by dotted lines. Note that the dihedral angle in the protein simulations remains in the range  $[-140^\circ, -90^\circ]$ .



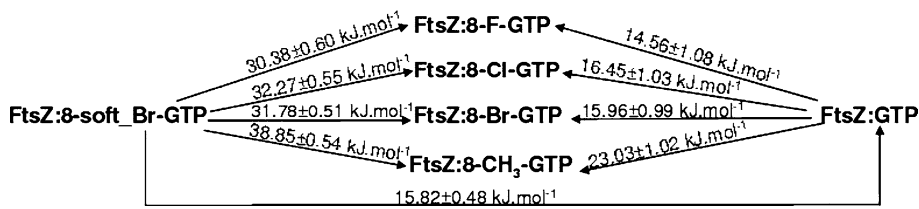


**Fig. 3** Thermodynamic cycles used to calculate the free energy difference between compounds in complex with FtsZ protein. The free energy differences between the reference compound (8-soft\_Br-

GTP) and the real compounds were calculated by OS using the perturbation formula (Zwanzig 1954). The free energies relative to GTP were obtained by cycle closure

**Table 1** Comparison of binding affinities to FtsZ protein for C8-substituted GTP analogs with respect to GTP as obtained from computational simulations,  $\Delta\Delta G_{\text{GTP,R}}^{\text{calc}}(\text{bind})$ , and corresponding

	$\Delta G_{\text{GTP,R}}^{\text{OS}}(\text{FtsZ}) (\text{kJ mol}^{-1})$	$\Delta G_{\text{GTP,R}}^{\text{ES-OS}}(\text{aq}) (\text{kJ mol}^{-1})$	$\Delta\Delta G_{\text{GTP,R}}^{\text{calc}}(\text{bind}) (\text{kJ mol}^{-1})$	$\Delta\Delta G_{\text{GTP,R}}^{\text{exp}}(\text{bind}) (\text{kJ mol}^{-1})$
GTP	0	0	0	0
8-F-GTP	$14.6 \pm 1.1$	$15.0 \pm 1.4$	$-0.8 \pm 2.5$	—
8-Cl-GTP	$16.5 \pm 1.0$	$12.8 \pm 1.3$	$3.7 \pm 2.3$	$8.0 \pm 4.4$
8-Br-GTP	$16.0 \pm 1.0$	$5.9 \pm 1.3$	$10.1 \pm 2.3$	$9.2 \pm 1.8$
8-CH <sub>3</sub> -GTP	$23.0 \pm 1.0$	$12.6 \pm 1.4$	$10.5 \pm 2.4$	$\sim 8.7^a$

Values of free energy differences in complex with FtsZ relative to GTP ( $\Delta G_{\text{GTP,R}}^{\text{OS}}(\text{FtsZ})$ ) were derived from the thermodynamic cycles shown in Fig. 3 based on the calculated values by OS free energy perturbation calculations. Relative free energy values in explicit water,  $\Delta G_{\text{GTP,R}}^{\text{ES-OS}}(\text{aq})$ , were calculated by the ES-OS method (Hritz and Oostenbrink 2009)

<sup>a</sup> Value for  $\Delta\Delta G_{\text{GTP,8-CH}_3-\text{GTP}}^{\text{exp}}(\text{bind})$  was estimated from an experimental 50% inhibition concentration (IC<sub>50</sub>) value of GTPase activity

affinities. The computationally predicted values are compared with the last column in Table 1, which lists the only available experimental binding affinities, to *Methanococcus jannaschii* FtsZ (Läppchen et al. 2008). We do not expect that the binding affinities will deviate significantly between *M. jannaschii* FtsZ and *A. aeolicus* FtsZ, since X-ray structures of FtsZ from both species show very similar monomer interfaces, which comprise the nucleotide binding pocket (Oliva et al. 2007). Moreover, for both proteins it was observed that different ligands do not lead to different conformation of the binding site (Oliva et al. 2007).

## Discussion

The calculated relative binding affinities of C8-substituted GTP analogs to the FtsZ protein compare well to the experimental values, with root-mean-square error of  $2.7 \text{ kJ mol}^{-1}$  for 8-Cl-GTP, 8-Br-GTP, and 8-CH<sub>3</sub>-GTP. Note that no empirical parameters, other than the force field to calculate the interactions, were used to obtain these values. Table 1 nicely illustrates that the relative free energies in both environments are equally important for the final free energies. The bromine and methyl substituent are both predicted to be much weaker binders with respect to chloride, by roughly  $\sim 6.5 \text{ kJ mol}^{-1}$ . However, while the dominant contribution to this difference comes from the

water environment for 8-Br-GTP, it comes from the bound state for 8-Me-GTP. It is also interesting to note that the GTP analog that is predicted to have the highest affinity is 8-F-GTP, resulting from similar contributions in both environments. No experimental data is available for this compound, as difficulties concerning its synthesis were only recently resolved (Liu et al. 2006; Ghosh et al. 2007).

It is usually considered that the *anti* conformation corresponds to a low and the *syn* conformation to a high value of the coupling constant,  ${}^3J(\text{C4},\text{H1}')$  (Stolarski et al. 1984; Cho and Evans 1991; Ippel et al. 1996; Trantirek et al. 2002). Therefore it may seem surprising that the ensemble average  $\langle {}^3J(\text{C4},\text{H1}') \rangle$  of GTP in water (to which the *syn* conformation contributes with  $\sim 3\%$ ) is calculated to be lower (2.4 Hz) than the value obtained for the bound state of GTP (2.95 Hz) in which only the *anti* conformation is observed (Fig. 2). This finding follows directly from the fact that within the FtsZ binding site the  $\chi$  dihedral angle is restricted within tighter bounds for all five C8-substituted GTP analogs as compared with in aqueous solution.

The paradigm of conformational selection describes the binding process between ligand and protein by taking multiple conformations of the protein into account. It states that the correct conformation is selected from the complete ensemble of possible conformations, which are all populated to a given extent (Carlson 2002). Here, we apply this model to the GTP analogs and quantify the contribution of

**Table 2** The free energy of restraining the conformation of C8-substituted GTP analogs to a conformational range  $\chi \in [-140^\circ, -90^\circ]$  in water

	$[\langle -140^\circ, -90^\circ \rangle]_{\text{(aq)}}^R$	$\Delta G_R^{\text{rest}}(\text{aq})$ (kJ mol $^{-1}$ )	$\Delta\Delta G_{\text{GTP},R}^{\text{rest}}(\text{aq})$ (kJ mol $^{-1}$ )
GTP	50%	1.7	0.0
8-F-GTP	48%	1.8	0.1
8-Cl-GTP	18%	4.2	2.5
8-Br-GTP	3.3%	8.4	6.7
8-CH <sub>3</sub> -GTP	4.0%	8.0	6.2

The free energy values  $\Delta G_R^{\text{rest}}(\text{aq})$  are calculated from the populations  $[\langle -140^\circ, -90^\circ \rangle]_{\text{(aq)}}^R$ . A comparison of the relative free energies with respect to GTP,  $\Delta\Delta G_{\text{GTP},R}^{\text{rest}}(\text{aq})$ , indicates a significant contribution to the total relative binding affinity,  $\Delta\Delta G_{\text{GTP},R}^{\text{calc}}(\text{bind})$  (Table 1)

the conformational restriction to the relative binding affinities. For this, we calculate the free energy that is needed to restrict the GTP analogs from their unbound state to a conformation that is possible in the protein, using Eq. 7.

$$\Delta G_R^{\text{rest}}(\text{aq}) = -kT \ln [\langle -140^\circ, -90^\circ \rangle]_{\text{(aq)}}^R, \quad (7)$$

where the unitless populations  $[\langle -140^\circ, -90^\circ \rangle]_{\text{(aq)}}^R$  were obtained from a simple integration over the selected range of a normalized dihedral angle distribution of compound  $R$  in water (solid lines in Fig. 2). The relative values with respect to GTP in water,  $\Delta\Delta G_{\text{GTP},R}^{\text{rest}}(\text{aq})$ , are listed in the fourth column of Table 2. It is interesting to note that these follow the same trend as the  $\Delta\Delta G_{\text{GTP},R}^{\text{calc}}(\text{bind})$  values (Table 1, fourth column). It seems that the conformational restriction of the GTP analogs accounts for roughly 65% of the difference in affinity for the FtsZ protein. We emphasize that, while the calculation of  $\Delta\Delta G_{\text{GTP},R}^{\text{calc}}(\text{bind})$  requires extensive simulations in water and in the binding site of the FtsZ protein, the restraining free energy values were calculated from a simple integration of dihedral angle distributions obtained from the water simulation only. Our results strongly indicate that the previously reported correlation between the binding affinities and Sterimol B1 parameter of the substituents (Läppchen et al. 2008) follows from the differences in the restraining free energies of the GTP analogs, which in turn stem from a different *syn-anti* balance of the compounds, when free in solution.

In agreement with the experimental observations, all compounds adopt roughly the same conformation when bound to the protein, while the various substituents lead to different conformational ensembles when the compounds are free in solution. The conformational restriction upon binding to the FtsZ protein accounts for roughly 65% of the differences in binding affinity. As the binding affinity seems to be for a large part dependent on the conformational ensemble of the studied C8-substituted GTP analogs

in water, a low specificity may be expected against other GTPases in which the binding site restricts the conformational freedom of C8-substituted GTP analogs in a similar manner. The inhibitory activities for such proteins will presumably display the same trend. A notable exception is tubulin, the eukaryotic homolog of FtsZ, where GTP analogs with small C8 substituents promoted assembly more than GTP itself.

## Conclusions

Relative free energy differences of five C8-substituted GTP analogs in complex with the bacterial cell-division protein FtsZ were calculated using the one-step perturbation (OS) method. Combined with previous values for the water environment as obtained from enhanced sampling OS we calculated the relative binding free energies for these compounds. The results are in good agreement with the available experimental binding affinities. The dihedral angle distributions within the FtsZ binding site are much narrower as compared with those obtained in water. This results in significantly different ensemble averages of the  $^3J$  coupling constants.

The contribution of conformational selection for the C8-substituted GTP analogs was quantified by calculating the restraining free energy in water that is needed to restrain the dihedral angle to the conformational range that is accessible within the binding site of the FtsZ protein. The restraining free energies follow the same trend as the binding free energies, accounting for about 65% of the differences in affinity. This suggests low specificity towards the FtsZ protein, because the same trend can be expected for any GTPases in which the binding site restricts the conformational freedom of C8-substituted GTP analogs in a similar manner. Our results also suggest an explanation for the empirically observed correlation between the Sterimol parameters and the binding affinity to the FtsZ protein.

**Acknowledgments** We gratefully acknowledge financial support from the Netherlands Organization for Scientific Research (NWO), Horizon Breakthrough grant 935.18.018 (J.H.) and VENI grant 700.55.401 (C.O.).

**Open Access** This article is distributed under the terms of the Creative Commons Attribution Noncommercial License which permits any noncommercial use, distribution, and reproduction in any medium, provided the original author(s) and source are credited.

## References

- Adams DW, Errington J (2009) Bacterial cell division: assembly, maintenance and disassembly of the Z-ring. Nat Rev Microbiol 7:642–653

- Berendsen HJC, Postma JPM, van Gunsteren WF, Hermans J (1981) Interaction models for water in relation to protein hydration. In: Pullman B (ed) Intermolecular forces. Reidel, Dordrecht, pp 331–342
- Berendsen HJC, Postma JPM, van Gunsteren WF, DiNola A, Haak JR (1984) Molecular-dynamics with coupling to an external bath. *J Chem Phys* 81:3684–3690
- Berman HM, Henrick K, Nakamura H (2003) Announcing the worldwide Protein Data Bank. *Nat Struct Biol* 10:980
- Beutler TC, Mark AE, van Schaik RC, Gerber PR, van Gunsteren WF (1994) Avoiding singularities and numerical instabilities in free energy calculations based on molecular simulations. *Chem Phys Lett* 222:529–539
- Carlson HA (2002) Protein flexibility and drug discovery: how to hit a moving target. *Curr Opin Chem Biol* 6:447–452
- Chen YD, Erickson HP (2009) FtsZ filament dynamics at steady state: subunit exchange with and without nucleotide exchange. *Biochemistry* 48:6664–6673
- Cho BP, Evans FE (1991) Correlation between nmr spectral parameters of nucleosides and its implication to the conformation about the glycosyl bond. *Biochem Biophys Res Commun* 180:273–278
- Christen M, Hunenberger PH, Bakowies D, Baron R, Burgi R, Geerke DP, Heinz TN, Kastenholz MA, Krautler V, Oostenbrink C, Peter C, Trzesniak D, Van Gunsteren WF (2005) The GROMOS software for biomolecular simulation: GROMOS05. *J Comput Chem* 26:1719–1751
- Czaplewski LG, Collins I, Boyd EA, Brown D, East SP, Gardiner M, Fletcher R, Haydon DJ, Henstock V, Ingram P, Jones C, Noula C, Kennison L, Rockley C, Rose V, Thomaides-Brears HB, Ure R, Whittaker M, Stokes NR (2009) Antibacterial alkoxybenzamide inhibitors of the essential bacterial cell division protein FtsZ. *Bioorg Med Chem Lett* 19:524–527
- Davies DB (1978) Conformations of nucleosides and nucleotides. *Progress Nucl Magn Res Spectr* 12:135–225
- Ghosh A, Lagisetty P, Zajc B (2007) Direct synthesis of 8-fluoro purine nucleosides via metalation-fluorination. *J Org Chem* 72:8222–8226
- Haydon DJ, Stokes NR, Ure R, Galbraith G, Bennett JM, Brown DR, Baker PJ, Barynin VV, Rice DW, Sedelnikova SE, Heal JR, Sheridan JM, Aiwale ST, Chauhan PK, Srivastava A, Taneja A, Errington J, Czaplewski LG (2008) An inhibitor of FtsZ with potent and selective anti-staphylococcal activity. *Science* 321:1673–1675
- Hockney RW (1970) The potential calculations and some applications. *Meth Comput Phys* 9:136–211
- Hritz J, Oostenbrink C (2007) Optimization of replica exchange molecular dynamics by fast mimicking. *J Chem Phys* 127:204104
- Hritz J, Oostenbrink C (2008) Hamiltonian replica exchange molecular dynamics using soft-core interactions. *J Chem Phys* 128:144121
- Hritz J, Oostenbrink C (2009) Efficient free energy calculations for compounds with multiple stable conformations separated by high energy barriers. *J Phys Chem B* 113:12711–12720
- Huang Q, Tonge PJ, Slayden RA, Kirikae J, Ojima I (2007) FtsZ: a novel target for tuberculosis drug discovery. *Curr Top Med Chem* 7:527–543
- Ippel JH, Wijmenga SS, de Jong R, Heus HA, Hilbers CW, de Vroom E, van der Marel GA, van Boom JH (1996) Heteronuclear scalar couplings in the bases and sugar rings of nucleic acids: their determination and application in assignment and conformational analysis. *Magn Reson Chem* 34:S156–S176
- Kapoor S, Panda D (2009) Targeting FtsZ for antibacterial therapy: a promising avenue. *Exp Opin Ther Targets* 13:1037–1051
- Karplus M (1959) Contact electron-spin coupling of nuclear magnetic moments. *J Chem Phys* 30:11–15
- Läppchen T (2007) Synthesis of GTP analogues and evaluation of their effect on the antibiotic target FtsZ and its eukaryotic homologue tubulin. PhD thesis, University of Amsterdam (available online <http://dare.uva.nl/en/record/211017>); Chapter 3
- Läppchen T, Hartog AF, Pinas VA, Koomen GJ, den Blaauwen T (2005) GTP analogue inhibits polymerization and GTPase activity of the bacterial protein FtsZ without affecting its eukaryotic homologue tubulin. *Biochemistry* 44:7879–7884
- Läppchen T, Pinas VA, Hartog AF, Koomen GJ, Schaffner-Barbero C, Andreu JM, Trambaiolo D, Löwe J, Juhem A, Popov AV, den Blaauwen T (2008) Probing FtsZ and tubulin with C8-substituted GTP analogs reveals differences in their nucleotide binding sites. *Chem Biol* 15:189–199
- Liu HY, Mark AE, van Gunsteren WF (1996) Estimating the relative free energy of different molecular states with respect to a single reference state. *J Phys Chem* 100:9485–9494
- Liu J, Barrio J, Satyamurthy N (2006) Kinetics and mechanism of the defluorination of 8-fluoropurine nucleosides in basic and acidic media. *J Fluor Chem* 127:1175–1187
- Lock RL, Harry EJ (2008) Cell-division inhibitors: new insights for future antibiotics. *Nat Rev Drug Discov* 7:324–338
- Löwe J, Amos LA (1998) Crystal structure of the bacterial cell-division protein FtsZ. *Nature* 391:203–206
- Mendieta J, Rico AI, Lopez-Vinas E, Vicente M, Mingorance J, Gomez-Puertas P (2009) Structural and functional model for ionic ( $K^+/\text{Na}^+$ ) and pH dependence of GTPase activity and polymerization of FtsZ, the prokaryotic ortholog of Tubulin. *J Mol Biol* 390:17–25
- Michie KA, Lowe J (2006) Dynamic filaments of the bacterial cytoskeleton. *Ann Rev Biochem* 75:467–492
- Oliva MA, Cordell SC, Löwe J (2004) Structural insights into FtsZ protofilament formation. *Nat Struct Mol Biol* 11:1243–1250
- Oliva MA, Trambaiolo D, Löwe J (2007) Structural insights into the conformational variability of FtsZ. *J Mol Biol* 273:1229–1242
- Oostenbrink C, van Gunsteren WF (2004) Free energies of binding of polychlorinated biphenyls to the estrogen receptor from a single simulation. *Proteins* 54:237–246
- Oostenbrink C, van Gunsteren WF (2005) Free energies of ligand binding for structurally diverse compounds. *Proc Natl Acad Sci U S A* 102:6750–6754
- Oostenbrink C, Villa A, Mark AE, van Gunsteren WF (2004) A biomolecular force field based on the free enthalpy of hydration and solvation: the GROMOS force-field parameter sets 53A5 and 53A6. *J Comput Chem* 25:1656–1676
- Paradis-Bleau C, Beaumont M, Sanschagrin F, Voyer N, Levesque RC (2007) Parallel solid synthesis of inhibitors of the essential cell division FtsZ enzyme as a new potential class of antibiotics. *Bioorg Med Chem* 15:1330–1340
- Romberg L, Mitchison TJ (2004) Rate-limiting guanosine 5'-triphosphate hydrolysis during nucleotide turnover by FtsZ, a prokaryotic tubulin homologue involved in bacterial cell division. *Biochemistry* 43:282–288
- Ryckaert J-P, Ciccotti G, Berendsen HJC (1977) Numerical integration of cartesian equations of motion of a system with constraints: molecular dynamics of n-alkanes. *J Comput Phys* 23:327–341
- Schäfer H, van Gunsteren WF, Mark AE (1999) Estimating relative free energies from a single ensemble: hydration free energies. *J Comput Chem* 20:1604–1617
- Stolarski R, Hagberg CE, Shugar D (1984) Studies on the dynamic syn-anti equilibrium in purine nucleosides and nucleotides with the aid of  $^1\text{H}$  and  $^{13}\text{C}$  NMR spectroscopy. *Eur J Biochem* 138:187–192

- Tadros M, Gonzalez JM, Rivas G, Vicente M, Mingorance J (2006) Activation of the *E. coli* cell division protein FtsZ by low affinity interaction with monovalent cations. FEBS Lett 580:4941–4946
- Tironi IG, Sperb R, Smith PE, van Gunsteren WF (1995) A generalized reaction field method for molecular-dynamics simulations. J Chem Phys 102:5451–5459
- Trantirek L, Stefl R, Masse JE, Feigon J, Sklenar V (2002) Determination of the glycosidic torsion angles in uniformly C-13-labeled nucleic acids from vicinal coupling constants 3 J(C2/4–H1') and 3 J(C6/8–H1'). J Biomol NMR 23:1–12
- Vollmer W (2006) The prokaryotic cytoskeleton: a putative target for inhibitors and antibiotics? Appl Microbiol Biotech 73:37–47
- Zwanzig RW (1954) High-temperature equation of state by a perturbation method. I. Nonpolar gases. J Chem Phys 22:1420–1426